한국동력기계공학회지 제10권 제4호 pp.90~98 2006년 11월

A Fatigue Analysis of the Common Stand in a Steel Mill through the Evaluation of Thermal Effects
열영향 평가를 통한 제철공장 공동가대의 피로해석

Y. K. Park and J. G. Kim
박용국·김진곤

Key Words : Common Stand(공동가대), Steel Mill(제철공장), Heatproof Plate(방열판), Stress Analysis(응력해석), High Cycle Fatigue(고주기피로), Mean Stress Effect(평균응력효과)

Abstract : 본 연구에서는 체철공장에서 래이들 카의 매우 높은 열에 주기적으로 빈번히 노출되는 공동가대의 열적 피해에 대한 체계적인 평가를 수행하였다. 먼저 실험과 함께 유한요소법을 사용한 열해석이 수행되었다. 기존 공동가대와 향후 설치될 신 공동가대 모두에 대한 적합한 기준을 검증하기위하여 가장 심각한 상태에 대한 열평가가 포함되었다. 또한 공동가대에 적합한 방열판의 설계를 위하여 실험결과에 근거한 수치해석이 사용되었다. 마지막으로 새로 설치될 공동가대의 안전성과 내구성을 평가하기위한 피로해석을 수행하였다. 6m 신형공동가대의 열응력해석 및 피로해석 결과 기존 공동가대보다는 취약하나 설치 및 사용에는 문제가 없음을 확인하였다.

1. 서 론

In a steel mill, common stands reside directly above a railway on which ladle cars or torpedo cars carrying high temperature molten steel pass frequently and periodically. Numerous pipes and cables, such as vapor pipes, power and data cables, are supported by a common stand as shown in Fig. 1.[1] Since the cables are highly susceptible to thermal damages, an ambient temperature should be below 60 °C. Thus, it is imperative to properly protect a common stand from excessive heat of a ladle car passing under it. A common stand is usually located at 12 meters above the ground. Consequently, it is unlikely for the common stand to suffer any serious heat damages even when a ladle car accidentally halts and remains directly under it for an extended duration of time by some malfunction.

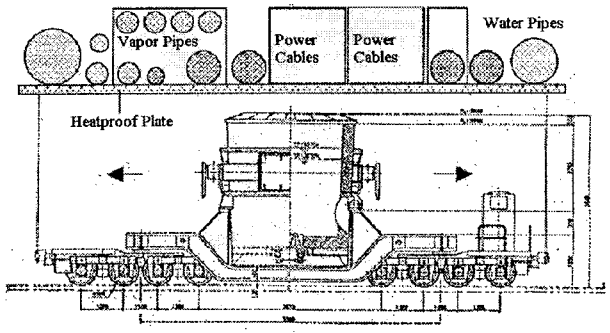

Fig. 1 A common stand over a ladle car on a railway in a steel mill

However, since a newly designed common stand will be built above only 6 meters from the ground, unexpected stoppage of a ladle car on a railway can induce a catastrophic outcome to the common stand. Accordingly, we are demanded to devise a reliable methodology in order to assure a new low-height common stand not to be subjected to hostile heat environment. Another important issue entailed by repetitive exposures to extreme heat is thermal fatigue of a common stand, which may jeopardize its structural integrity. In essence, the safety of a common stand is not to be compromised. For this goal,

접수일 : 2006년 8월 10일, 채택확정 : 2006년 9월 18일
박용국(책임저자) : 대구가톨릭대학교 기계자동차공학부
E-mail : ykpark@cu.ac.kr Tel. 053-850-2723
김진곤 : 대구가톨릭대학교 기계자동차공학부

thermal analysis of a common stand and development of a heatproof system are prerequisite. And they should be followed by fatigue analysis.

To develop a heat transfer model for the entire system, we first build a steady-state heat transfer model. Measurement of the temperature of a ladle car and an ambient temperature is also necessary for numerical analyses. Afterwards, a suitable heatproof plate is selected and adopted to protect a new common stand. Thermal stresses from uneven temperature distributions are also calculated. Lastly, a fatigue analysis is performed to estimate the accumulated damage of the new common stand from repeated thermal stress and to evaluate its safety.

2. Thermal Analysis of a Heatproof System

The objective of this section is twofold: rudimentary analysis to build a proper heat transfer model of a common stand, and evaluation of aptitude of the current and new heatproof plates.

2.1 Preliminary thermal analysis of the current heatproof plate for a common stand

In reality, a heatproof plate is installed under a common stand to block the heat and protect it in case a ladle car (a heat source) jeopardizes the safety of a common stand. Based on the past experience, the current 12-meter, heatproof plate-clad common stand has not confronted any serious thermal problems in the steel mill. However, it should be tested whether the current heatproof plate suffices for the new low-height common stand. The dimension and materials of the existing heatproof plate are presented in Table 1.

Table 1 Dimension and materials of the existing heatproof plate

Structure	Material	Dimension [mm]
Top plate	Steel	1000x1000x3.2
Middle plate	Unknown	1000x1000x60.0
Bottom plate	Steel	1000x1000x2.0

Unfortunately enough, however, the thermal characteristics of the sandwich-type heatproof plate are not available except that of steel. For the estimation of its thermal properties, we raise the temperature of the bottom of a heatproof plate to 375 °C according to the new protocol for field use, and check the top surface temperature at an ambient temperature of 10°C. Under this condition, the new protocol requires the top surface temperature of a heatproof plate should be lower than 60°C to guarantee the safety of a common stand. And using ANSYS[2], we may calculate thermal properties of the current heatproof plate, such as thermal conductivity and heat transfer coefficient. Also, we can check the aptitude or insulation capability of the current heatproof plate for a new common stand.

When a flat plate is horizontally laid, and is bottom-heated and cooled on top in air, it can be modeled as a free or natural convection problem.[3]

$$\overline{Nu}_L = \frac{\bar{h}L}{k} = 0.15 Ra_L^{1/3} \quad (10^7 \le Ra_L \le 10^{11}) \tag{1}$$

where $Ra_L = \frac{g\beta(T_s - T_\infty)L^3}{\nu\alpha}$ In Eq. (1), heat transfer coefficient 'h' of 9.1 [W/m^{2}K] was obtained from correlations suggested by several researchers.[4)-6)] Employing this value for a heat transfer coefficient, we then vary the thermal conductivity (k) of unknown material in the heatproof plate from 1 to 20 [W/mK] in order to calculate the top surface temperature by ANSYS. For 'k'=1, 10, and 20, the top surface temperature is 266.9 °C, 360.0 °C and 367.2 °C respectively. Fig. 2 shows the top surface temperature in the case of thermal conductivity of 1 [W/mK]. Now, fixing the thermal conductivity as 1[W/mK], we change the heat transfer coefficient to 28, 56, 112 [W/m2K] and calculate the top surface temperature. This time, the top surface temperature is 146.0 °C, 93.6 °C and 58.7 °C respectively. Table 2 summarizes the entire

ANSYS results. Only for the highest value of 'h'=112 [W/m2K], the top surface temperature is below 58.7 °C and satisfies the requirement of the new protocol for a heatproof plate. However, a heat transfer coefficient of 112 is regarded unreasonably high for free convection and 'h' value of 9.1 from Eq. (1) is much more pertinent or convincing.

Since no experimental measurement was performed, we do not ascertain the thermal conductivity of the unknown material. Nevertheless, no proof beyond a reasonable doubt is present that 'h' value of 9.1[W/m2K] is inaccurate in excess.

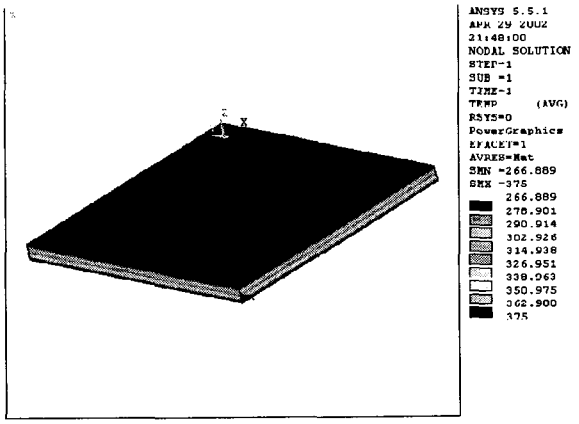

Fig. 2 Calculated temperature of the current heatproof plate (k=1[W/mK])

Table 2 Temperature of the top surface of the old heatproof plate [oC]

h	k	Temp.	k	h	Temp.
9.1	1	266.9	1	28	146.0
	10	360.0		56	93.6
	20	367.2		112	58.7

Thus, the maximum allowed temperature of 60°C can be hardly attained for the current heatproof plate. In other words, the old plate dose not guarantee the safety or proper protection of a new low-height common stand against the extreme heat source of a ladle car. Although it has not caused any serious thermal damage to the 12-meter common stand in the past, therefore, it cannot be applicable to a new common stand. For a heatproof plate to be employed under the new protocol, the thermal conductivity 'k' is regarded to be much lower than 1 [W/mK]. As a result, the old heatproof plate was discarded by managerial decision on the field. Considering the previous calculation does not include any heat transfer via thermal radiation, we move to a next phase involving experimentation and calculation with radiation for a newly developed heatproof plate.

2.2 Thermal analysis of a new heatproof plate for a common stand

A new heatproof plate is to be designed for the 6-meter, low-height common stand by design engineers on the field. Table 3 and 4 show the dimensions, materials and properties of the new heatproof plate. And its aptitude is to be tested for use before adoption on the field. The heatproof plate and common stand are applied by heat flux of thermal radiation from a ladle car. Inside of them, heat transfer occurs by conduction, and they lose heat via convection heat transfer from the motion of ambient air and radiation. Thus, it becomes a complex heat transfer problem encompassing conduction, convection and radiation, and can be expressed as follows.[7)]

$$q = -k\frac{dT}{dx} \tag{2}$$

$$q = h(T_S - T_a) \tag{3}$$

$$q = \varepsilon\sigma(T_s^4 - T_a^4) \tag{4}$$

where, k: thermal conductivity,
h : heat transfer coefficient,
ε : emissivity,
σ : Stefan-Boltzmann constant,
T_s : surface temperature of a structure, and
T_a : ambient temperature

Therefore, the total heat lost is the sum of heat transferred by radiation and convection.

$$H_{total} = H_{radiation} + H_{convection} \quad (5)$$

Table 3 Dimension and materials of a new heatproof plate

Structure	Material	Dimension [mm]
Top plate	Aluminum	1000x1000x0.5
Middle plate	SuperLite LW	1000x1000x60.0
Bottom plate	SS400 steel	1000x1000x3.2

Table 4 Thermophysical properties of SuperLite LW

Density [kg/m^3]	150
Thermal conductivity [W/mK]	0.056
Linear thermal expansion [%]	1.4

To establish an appropriate heat transfer model and confirm the validity of the model, finite element analyses of the model are conducted in parallel with experiments. First, according to the new protocol for a heatproof plate, we perform experiments to heat the heatproof plate on the bottom and measure the top surface temperature in an ambient temperature of 10 °C. The bottom surface is heated to be 375 °C because, according to the new protocol, it is the maximum temperature of the bottom surface assuming an exposure of a common stand to an extreme heat source. The bottom of the plate is also heated up to steady state temperatures of 230 and 175 °C to establish a heat transfer model with a more consistent accuracy. Fig. 3 exhibits the temperature change of the bottom surface of the plate until it reaches a thermal steady state. In the experiments, when the top surface reaches 375.9, 230.0 and 174.7°C in a steady state, the corresponding top surface temperature of the heatproof plate is measured. And they are illustrated in Fig. 4. We can observe the highest temperature is 60.7 °C and sequentially followed by 38.1 and 29.3°C.

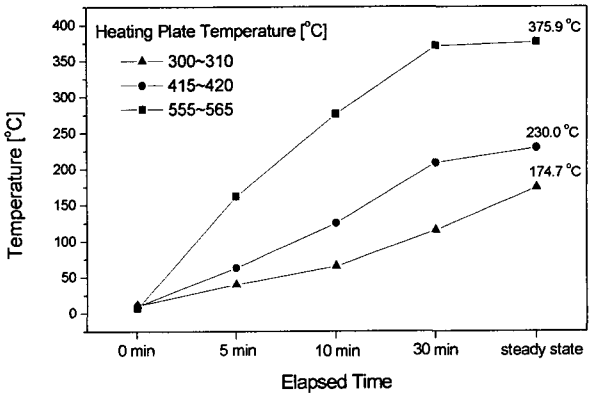

Fig. 3 Temperature of the heatproof plate (bottom surface)

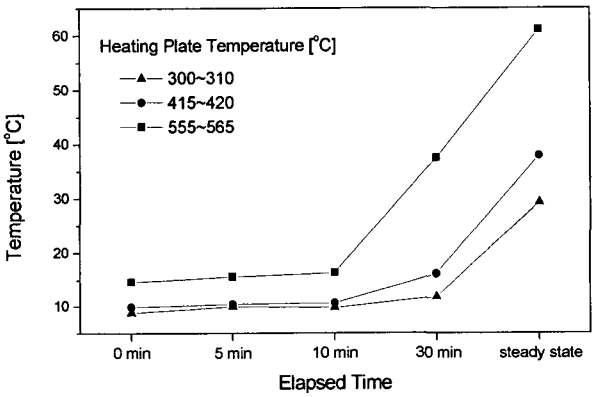

Fig. 4 Temperature of the heatproof plate (top surface)

A finite element model is adopted to predict the experimental results using an appropriate heat transfer model and thus to validate its accuracy. First, using ANSYS, with emissivity(surface radiative property) of 0.5, the top surface temperature and heat flux are calculated on the condition of the ambient temperature being 10 °C. When the plate bottom is heated to 375 °C, the top surface is calculated to be 83 °C and the heat flux is 273 [Watt]. It shows a fairly large discrepancy from the actual measurement of 60.7 °C. Meanwhile, when 0.7 is used for emissivity instead of 0.5, the top surface is calculated to be 68 °C and the heat flux is 282 [Watt]. With emissivity of 0.7, therefore, the

ANSYS model predicts the actual temperature more accurately.

Comparing the temperature 68 °C from ANSYS model with the actual measurement in the experiment, 60.7 °C, we notice the temperature predicted by ANSYS is still slightly higher than the top surface temperature measured. Since the heatproof plate also experiences additional heat loss via convection in reality, we consider the accuracy of calculation is not greatly unsatisfactory. In fact, because the experiment is conducted in a closed environment absolutely blocking airflow from outside, convectional heat transfer is presumed to be relatively small.

Using the last heat transfer model including both convection and radiation with emissivity of 0.7, based on the bottom temperature of 370°C, we ultimately obtain 60.1°C as a top surface temperature of the plate. This ANSYS result is almost identical to the actual measurement of 60.7°C. To further confirm the validity and accuracy of this final heat transfer model, we duplicate calculations of top surface temperatures while varying bottom surface temperatures (230°C and 175°C). The ANSYS results are compared with actual measurements in Table 5. The top surface temperatures predicted by ANSYS in column 3 roughly coincide with those measured inexperiments in column 2. Hence, the accuracy of the heat transfer model is reasonably high. The last column in Table 5 is ANSYS results based on the ambient temperature of 35°C, which is highly probable on a hot summer day. In fact, a top surface temperature of 73.3°C in the most extreme case is out of the temperature tolerance range defined in the new protocol. Since the heatproof plate can be installed apart from the bottom of a common stand instead of being directly attached to it, however, it is not considered as dangerous as it may look. In conclusion, the performance of a new heatproof plate conforms to the insulation specification of the 6-meter, low-height common stand. And the management decided to adopt this new heatproof plate for actual field use.

Table 5 Finite element analysis result vs. temperature measured experimently [℃]

Bottom surface (measured)	Experiment	ANSYS	
	Top surface (ambient temp. of 10 °C)		Top surface (ambient temp. of 35 °C)
375.9	60.7	60.1	73.3
230.0	38.1	39.9	58.0
174.7	29.3	31.3	51.8

3. Thermal and Stress Analyses of a Common Stand

In this section, we develop a thermal analysis model for the entire common stand system including the heat transfer model of a heatproof plate in the previous section, of which its validity is already proven. The finite element model of the ladle car shown in Fig. 5 is constructed to accurately analyze the thermal effect of a ladle car containing 1650 °C molten steel (heat source) on a common stand. Also, to build a precise model, temperature of the side of the ladle car is measured. The temperatures of the top, middle and bottom of the ladle car side are measured twice and their average temperatures are obtained as 267, 403, and 274 °C respectively.

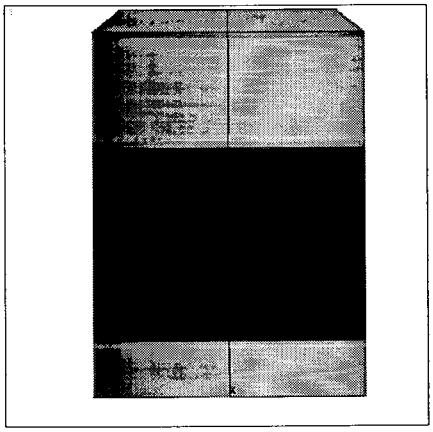

Fig. 5 Finite element model of a ladle car in a mini steel mill

Fig. 6 shows the temperature distribution of a new common stand without a heatproof plate above the ladle car modeled in Fig. 5. Fig 6 is different from Fig. 1 showing only the horizontal bridge of a common stand, on which pipes and cables are located. In reality, however, a common stand also has two vertical supports on each side of the railway as well as a horizontal bridge. In an ambient temperature of 35 °C, emulating a hot summer day, the bottom surface of the bridge is calculated to reach approximately 150 °C. As expected priorly, installation of a heatproof plate is imperative.

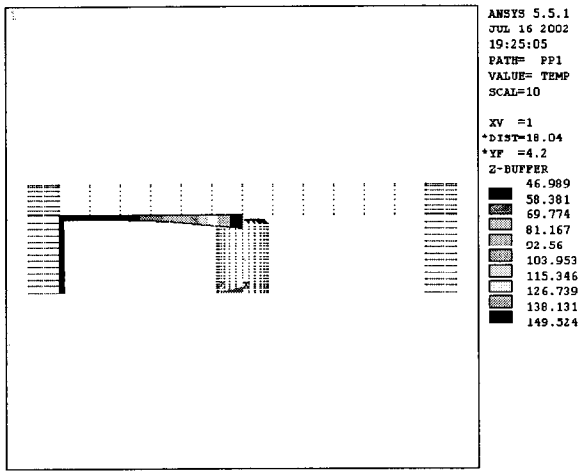

Fig. 6 Temperature distribution of a new common stand with no heatproof plate and a ladle car

In the ensuing analysis, taking account of the diameter of a typical ladle car and the width of a common stand bridge, we assume that a 6-meter long and 2-meter wide heatproof plate with identical materials and thermophysical properties in Table 3 and 4, is installed under a bridge (Fig. 7). To obtain a further grasp of the picture, a detailed temperature profile on the bottom surface of the left half of a bridge is presented in Fig. 8. With a proper protection of the 6x2 m2 heatproof plate, the temperature of a common stand bottom surface ranges between 41 and 63 °C, which can guarantee the safety of cables even in an ambient temperature of 35°C on a hot summer day. In consequence, this new heatproof plate is recommended for the field use.

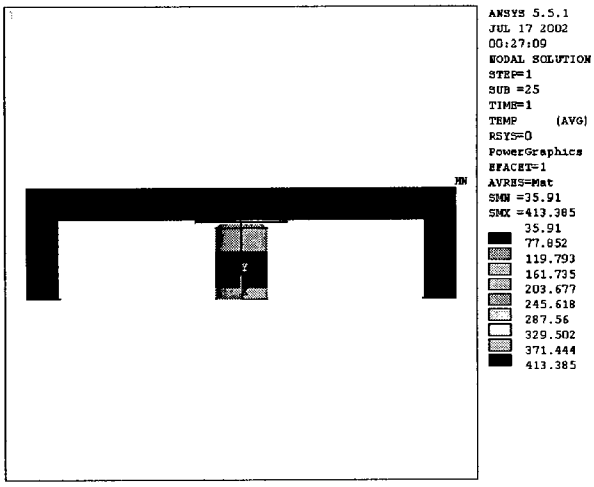

Fig. 7 Temperature distribution of a new common stand with a heatproof plate and a ladle car

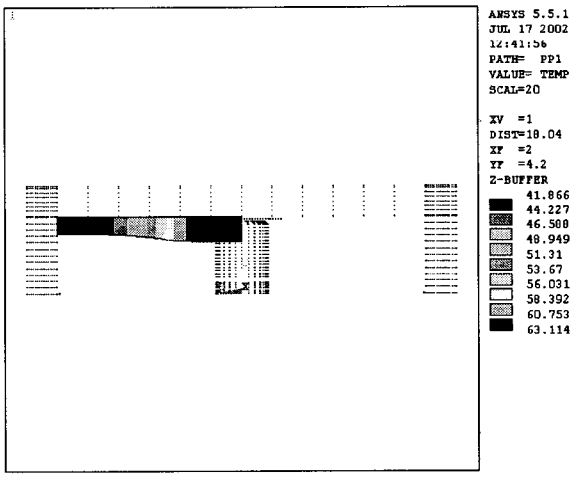

Fig. 8 Detailed temperature distribution of a common stand on the bottom surface (left half bridge only)

Based on the temperature distribution in a new common stand, a thermal-stress analysis is conducted by ANSYS. The stress distribution in the common stand is illustrated in Fig. 9. The maximum stress on the common stand is about 86.6 MPa. Due to the reduced distance from a ladle car, it is significantly greater than 50.3 MPa in the old common stand. However, it is still far short of the yield strength of 293 MPa or ultimate tensile strength of 421 MPa of the common stand

steel.[8] Hence, the structure is free from the danger of yielding or plastic deformation. Nonetheless, we cannot be positive that a repetitivestress does not induce any damage of a serious level to the structure. This is also a concern to the engineers on the field. To address this problem, the next section is devoted to a fatigue analysis of the common stand.

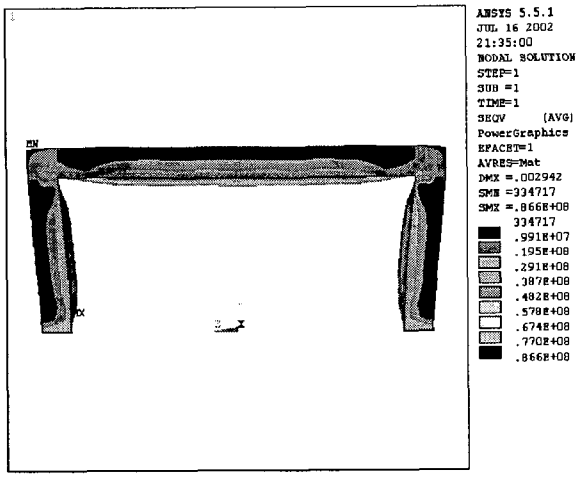

Fig. 9 Stress distribution in a newly designed common stand

4. Fatigue Analysis of a Common Stand

Once a common stand is constructed in a steel mill, it is supposed to last for an infinite duration of time until intentional destruction or retirement from service is determined. Since a new low-height common stand is substantially more proximate to the heat source of a ladle car passing through the common stand on a railway, it is exposed to repetitive thermal stresses or damages. Accordingly, it should be carefully assessed whether the safety of the structure is compromised or not in the aspect of a fatigue failure. If an infinite life of a common stand is not assured, an accurate calculation of its fatigue life (loading cycles to failure) has to be provided in the design stage. Consequently, a routine inspection in a predetermined period is demanded.

With the aid of a heatproof plate installed under the common stand to protect the structure, it is not likely to deteriorate at a rapid rate. Nevertheless, a long-term, cyclic thermal effect should not be ignored. Based on the heat transfer model and thermal stress analysis developed in the preceding sections, therefore, a reliable fatigue analysis is performed to evaluate the fatigue life of the common stand in this section. Since the maximum stress applied to the common stand is 86.6 MPa and significantly lower than the yield strength, it is primarily within the elastic range of the steel. In this situation, the resultant life is usually long and it belongs to high cycle fatigue. In high cycle fatigue, stress-life (or S-N) approach is prevalently adopted to understand the phenomenon and quantify fatigue life.[8),9)]

Table 6 is the S-N curve of structuralsteel, which signifies its fatigue life.[10)] As presented in the previous section, the maximum thermal stress in the common stand is 86.6 MPa. Thus, a stress amplitude(S) is 43.3 MPa. It is below a fatigue or endurance limit (Se) of 270 MPa in Table 6 assuming an infinite life of 10^6cycles to failure. Since an endurance limit is a stress level below which the common stand has an infinite life (over 10^6cycles to failure), the structure is safe against the fatigue failure.

In lieu of Table 6 or S-N curve method, also an empirical power relationship between stress(S) and life(N) can be used as Eq. (6).[11)]

Table 6 Fatigue life for the structural steel

Stress amplitude [MPa]	Number of cycles to failure
343	30,800
324	93,100
314	140,500
304	228,400
294	311,700
284	587,500
275	810,000
273	859,100
265	3,480,800

$$N = 10^{-C/b} S^{1/b} \quad \text{or} \quad S = 1.62UTS(N^{-0.0851}) \qquad (6)$$

where, $b = -\frac{1}{3}\log_{10}(S_{1000}/S_e)$, $C = \log_{10}(S_{1000}^{\ 2}/S_e)$

UTS is ultimate tensile strength, and S_{1000} is the alternating stress level corresponding to a life of 1,000 cycles. Since it is not directly available, it can be estimated as 0.9 times UTS or 379 MPa. The endurance limit S_e is 270 MPa. Using 270 MPa for stress amplitude applied, we can calculate the number of cycles to failure to be 10^6, which is considered as an infinite life for engineering purposes. Also, according to this relationship, the alternating stress level of 43.3 MPa in the common stand generates an identical result of 1.60 x 10^{22} cycles or infinite life.

The above S-N curve or power relationship of fatigue life is based on a rotating-uniform bending test in a laboratory. In other words, loading type of the fatigue test is fully reversed loading. The center of the cyclic alternating stress or mean stress is positioned at 0 MPa, or the maximum stress is tension and the minimum stress is compression of equal magnitude. In this case, the stress ratio (min/max) is 1 and the amplitude ratio (S/mean) is infinite. Meanwhile, for the cyclic loading in the common stand in reality, the stress ratio is 0 and the amplitude ratio is 1. Owing to this nonzero mean stress, there should be correction in the above relationship. In general, a positive mean stress is detrimental to a fatigue life because a fatigue crack propagates under in a tensile stress state.

To take the effect of nonzero mean stress into consideration, a few modifications are in use. Eq. (7) is Goodman's linear relationship, [12] which involves a relative term of mean stress over ultimate tensile strength of the material. For ductile steels, the true fracture strength is more relevant than UTS. Using UTS instead of the fracture strength, however, we can estimate the fatigue life of a common stand more conservatively. In fact, brittle steels are insensitive to either choice because UTS approaches the fracture strength.

$$\frac{S}{S_e} + \frac{\sigma_{mean}}{UTS} = 1 \qquad (7)$$

Since the maximum and minimum stresses in the new common stand are 86.6 and 0 MPa respectively, the mean stress is 43.3 MPa. Solving Eq. (7), $\frac{43.3}{S_n} + \frac{43.3}{421} = 1$. Thus, a modified stress amplitude(S_n) is 48.3 MPa, which is greater than the originalalternating stress of 43.3 MPa. Nonetheless, a limited increase in the stress amplitude does not significantly alter the expected fatigue life of the common stand. The number of cycles to failure is 1.72 x 10^{21}, which is still much larger than 10^6. In conclusion, the mean stress effect for fatigue failure of the common stand can be safely ignored

5. Conclusions

In this study, thermal analysis and durability test were performed for a new common stand to be constructed above a high temperature ladle car with molten steel regularly passing on a railway in a steel mill. Dissimilar to the existing common stand residing over 12 meters, the new one is considerably more proximate to the heat source and more susceptible to thermal stresses. With

the aid of ANSYS, a precise heat transfer model encompassing radiation and convection of heatproof system was firstly created. The accuracy of the model was confirmed by comparing the predicted temperatures with experimental data.

With a full FEM model of the common stand, the highest temperature of the common stand reached 150 °C. Upon deciding to adopt the improved heatproof plate of 6x2 m^2, we recalculated temperature distribution in the common stand assuming a hot summer day. The resultant temperature of 41-63 °C is low enough to warrant the safety of cables in the common stand. A thermal-stress analysis was subsequently conducted and the maximum stress applied to the common stand is 86.6 MPa. To further investigate this cyclic thermal loading would induce a fatigue failure to the structure, a high cycle fatigue analysis considering the effect of tensile mean stress was conducted. It indicates an alternating stress of 48.3 MPa is still below the endurance limit and an infinite fatigue life is guaranteed. Thus, the new common stand is robust against a long-term fatigue failure from repeated thermal loadings of high temperature ladle cars.

References

1. J. H. Kim, S. H. Park, S. H. and H. K. Wi, 1999, "A Study on the Efficiency Improvement of Railway Transportation in Molten Pig Iron Using Simulation", Journal of RIST, Vol. 13, No. 3, pp. 343-349.
2. ANSYS Analysis Guide, 2000, "ANSYS Release 6.0", SAS IP, Inc.
3. F. P. Incropera, D. P. DeWitt, 1990, "Introduction to Heat Transfer, 2nd ed", John Wiley and Sons, New York, pp. 500-506.
4. W. H. McAdmas, 1954, "Heat Transmission, 3rd ed", McGraw-Hill, New York.
5. R. J. Goldstein, E. M. Sparrow and D. C. Jones, 1973, "Natural Convection Mass Transfer Adjacent to Horizontal Plates", International Journal of Heat and Mass Transfer, Vol. 16, p. 1025.
6. J. R. Lloyd, and W. R. Moran, 1974, "Natural Convection Adjacent to Horizontal Surfaces of Various Platforms," ASME Paper 74-WA/HT-66.
7. S. V. Patankar, 1980, "Numerical Heat Transfer and Fluid Flow", Hemisphere Publishing Corp, New York, pp. 1-23.
8. K. Shiozawa, 1996, "Databook on Fatigue Strength of Metallic Materials", Elsevier Science B. V., Amsterdam, pp. 10-11.
9. T. Anderson, 1995, "Fracture Mechanics 2nd ed", CRC Press, London.
10. R. J. Sanford, 2003, "Principles of Fracture Mechanics", Prentice Hall, Upper Saddle River.
11. J. Bannantine, J. Comer and J. Handrock, 1990, "Fundamentals of Metal Fatigue Analysis", Prentice-Hall, Englewood Cliffs, pp. 4-5.
12. J. Collins, 1993, "Failure of Materials in Mechanical Design 2nd ed", John Wiley and Sons, New York, pp. 229-236.